

Kinetic aspects in the selectivity of deep hydrogenation of 2-ethylanthraquinone over Pd/SiO₂

A. Drelinkiewicz

Jagiellonian University, Faculty of Chemistry, Ingardena 3, 30-060 Cracow, Poland

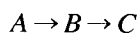
Received 7 October 1994; accepted 7 March 1995

Abstract

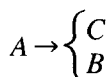
The liquid phase hydrogenation of 2-ethylanthraquinone (eAQ) was carried out in a slurry reactor in the presence of Pd/SiO₂ catalyst at atmospheric pressure of hydrogen in temperature range 18–62°C. 2-ethylanthrahydroquinone (eAQH₂) was initially formed with a selectivity close to 100%. In the further process termed ‘deep hydrogenation’ 2-ethyltetrahydroanthraquinone (H₄eAQ) was formed as the main product. eAQH₂ was also partly converted into other products, which were chromatographically separated and partly identified. A plausible reaction pattern including competitive (hydrogenation and hydrogenolysis) as well as consecutive reactions is postulated. Depending on the catalyst amount, grain size and temperature, deep hydrogenation was controlled by chemical reaction, internal diffusion or external mass transport processes. The influence of such different reaction regimes on the course of reaction and especially the yield of H₄eAQ has been discussed on the basis of the proposed reaction pattern. The highest yield of H₄eAQ was observed when reaction kinetics was controlled by external mass transport processes.

1. Introduction

In the case of hydrogenation reactions carried out in a 3-phase system the observed overall rate is often determined by the rate of mass-transport processes [1–3]. Most frequently it is hydrogen transport. In such systems catalysts are operating in a ‘hydrogen poor’ mode whereas those systems in which the overall reaction rate is mainly determined by the rate of chemical reaction are operating in a ‘hydrogen rich’ mode [4]. This concept is useful in correlating the effect of a reaction parameter (catalyst amount, temperature of reaction) with the selectivity of reaction. This correlation was discussed by Rylander [4] for the general type:



or



reactions where the rate equations for formation of B and C contain hydrogen concentration to different powers. The formation of the product for which the rate equation contains hydrogen concentration to a lower power will be favored by ‘hydrogen poor’ catalyst. The reverse holds for the other products. Two types of such competitive reactions are isomerisation and hydrogenation (fatty oils [5,6]) and hydrogenolysis and hydrogenation (ketones [7]). Both isomerisation and hydrogenolysis are favored in preference to hydrogenation by low hydrogen availability at the catalyst surface [4,6]. As an example of the consecutive reaction the reduction of nitrobenzene

Table 1
Characteristics of the sieve fractions of the catalyst

Grain size <i>d</i> (mm)	wt% Pd	Porosity (%)	Average predominant pore diameter (Å)
0.0675	4.00	53.6	89
0.11	4.04	39.6	89
0.135	4.06	41.7	84.7
0.175	3.99	35.0	86.2

was considered [8,9]. The parallel and consecutive reactions proceed in the course of the catalytic hydrogenation of anthraquinone [10] or its alkyl-derivative (2-ethyl)anthraquinone [11]. However this latter system is much more complex because the products of both reaction routes: hydrogenation and hydrogenolysis take part in many side processes and therefore several cosecutive reactions proceed simultaneously.

In the previous papers the present author studied the initial stage of 2-ethylanthraquinone (eAQ) reduction resulting in the relatively fast and selective hydrogenation (reaction 1 in Scheme 2) to 2-ethylanthrahydroquinone (eAQH₂) [11,12], analogously to the hydrogenation of quinones [13] and anthraquinones [10,14,15]. After the primary reduction (stage 'a') when transformation of eAQ into eAQH₂ became almost complete, a sharp decline of the rate of hydrogenation appeared [11,13,16,17]. Further hydrogenation (stage 'b') occurred with distinctly lower rate than in reaction 1 according to a very complicated reaction pattern (Scheme 2). Stage 'b' termed 'deep hydrogenation' is the object of the present research. In the course of 'deep hydrogenation' as the main product H₄eAQ was formed. The formation of H₄eAQ with high selectivity is required by technology in the anthraquinone method for hydrogen peroxide production [18]. All other products formed, termed 'degradation products' are undesirable from a technological point of view.

The aim of the present research was to study the products of 'deep hydrogenation' formed over Pd/SiO₂ catalyst, the effect of reaction conditions (catalyst amount and grain size, reaction temperature) as well as the effect of reaction regime

(diffusion or kinetically controlled process) on the course of the reaction. The discussion of all the obtained data enabled to propose the plausible reaction pattern presented in Scheme 2.

1.1. Abbreviations

eAQ	2-ethyl-9,10-anthraquinone
AQ	9,10-anthraquinone
eAQH ₂	2-ethyl-9,10-anthrahydroquinone
H ₄ eAQ	2-ethyltetrahydro-9,10-anthraquinone
H ₄ eAQH ₂	2-ethyltetrahydro-9,10-anthrahydroquinone
H ₆ eAQ	2-ethylhexahydro-9,10-anthraquinone
H ₈ eAQ	2-ethyloctahydro-9,10-anthraquinone
H ₈ eAQH ₂	2-ethyloctahydro-9,10-anthrahydroquinone
eAN	2-ethylanthrone
AN	anthrone
H ₄ eAN	2-ethyltetrahydroanthrone
H ₄ AN	tetrahydroanthrone
eANT	2-ethylanthracene
ANT	anthracene
H ₄ eANT	2-ethyltetrahydroanthracene
H ₄ ANT	tetrahydroanthracene

2. Experimental

2.1. Material used

2-Ethylanthraquinone (eAQ) was prepared in the Laboratory of Organic Chemistry, Jagiellonian University, Cracow. 2-Ethyl-5,6,7,8-tetrahydroanthraquinone (H₄eAQ) (m.p. 164°C) was prepared by catalytic hydrogenation of eAQ over 4% Pd/SiO₂-Al₂O₃, 2-ethylanthrone (eAN) (m.p. 60–61°C) was synthesized by the reduction of eAQ with Sn in acid solution [19]. It was identified using NMR, IR and mass-spectrometric analysis. 2-Ethylanthracene (eANT) was a commercial product (Aldrich).

2.2. Hydrogenation experiments

Solvents: a mixture of xylene–2-methylcyclohexyl acetate (1:1 volume ratio) was used. Before experiments solvents were purified as described earlier [12].

Catalyst: 4 wt% Pd supported on silica (BET surface area 320 m²/g) was applied. Fresh catalyst synthesized by a method described in [11] contained palladium oxide. After preparation the catalyst was separated on the several sieve fractions with average grain size *d*: 0.0675, 0.11, 0.135, 0.175 mm. The particular sieve fractions were characterized by determining the amount of palladium and determining pore structure using mercury porosimetry (Table 1). The distribution of palladium in the catalyst grains was studied using electron scanning microscope JEOL JXA-50 A and a Kevex X-ray microanalyser operating with the scanning microscope.

The catalyst was reduced in situ in the reactor immediately before the catalytic reaction [12].

Procedure: the hydrogenation experiments were carried out under agitated batch reactor conditions [12] at constant pressure of hydrogen equal to atmospheric pressure, in the temperature range 18–62°C. The kinetics of reaction was followed by measuring the volume of hydrogen consumed in reaction as a function of time. In the course of reaction the samples of solution (about 0.1 cm³) were taken at appropriate time intervals (15–20 min) and kept at ≈0°C before analysis. Hydrogenation experiments were carried out up to the consumption of 3.0–3.5 mol of hydrogen per 1 mol of eAQ initially present in the reactor. In a typical experiment 30 cm³ of eAQ solution and 0.3–0.9 g of catalyst was used.

2.3. Analytical methods

The composition of solution in the course of hydrogenation was analyzed by HPLC and TLC methods.

With HPLC at the conditions described earlier [12,20] (column: SiO₂, eluent: 2% isopropyl ether + 0.2% diglyme in n-heptane) concentration

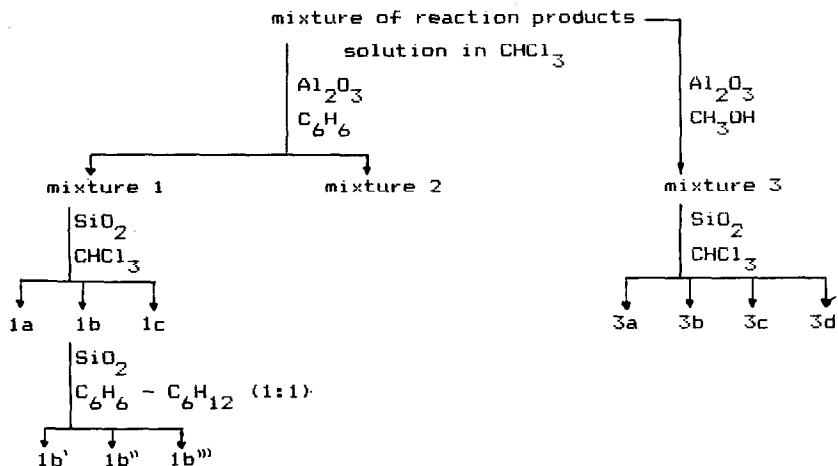
of eAQ and H₄eAQ was determined quantitatively while the presence of eAN, eANT and H₈eAQ only qualitatively. On HPLC chromatograms besides the peaks of the all above compounds some other peaks mostly of very low intensity and poorly separated were also observed.

With TLC analysis (SiO₂ coatings on alumina foil –commercial Aldrich, mobile phase: benzene) the presence of a few other side reaction products was observed. However they were not detectable by HPLC possibly due to their small concentration.

2.4. Separation and identification of the products of eAQ catalytic 'deep hydrogenation'

After the hydrogenation experiments the catalyst was filtered off. The remaining solution was oxygenated by air and H₂O₂ (the product of reaction between eAQH₂ or H₄eAQH₂ and oxygen) extracted with water. From the organic phase the solvents were separated by steam distillation. The distillation residue in the form of a yellow solid or of a red–brown oil was dissolved in CHCl₃ and dried over MgSO₄. From this solution the products of 'deep hydrogenation' were chromatographically separated as shown in Scheme 1. Using a column packed with Al₂O₃ and benzene as eluent two fractions 1 and 2 were obtained. However, in these conditions the adsorbed substances are only partially washed off from the column and partially remained at its head forming a red–brown ring. By applying additionally more polar solvent CH₃OH fraction 3 of the products was obtained. TLC and HPLC showed that fractions 1, 2 and 3 were in fact mixtures of different compounds. An attempt to separate them further was undertaken. For that purpose a column packed with SiO₂ and using CHCl₃ as the eluent were applied.

TLC and HPLC indicated that none of the eight fractions contained only a single substance. All of them were mixtures containing most frequently 2 or 3 compounds. The composition of individual fractions was analyzed using HPLC, TLC, NMR, IR and mass spectrometry. Not all hydrogenation



Scheme 1.

products of eAQ were identified. The following products were found:

H_4eAQ , H_6eAQ , H_8eAQ , $H_{10}eAQ$ –predominantly contained in mixture 2, eAN –mixture 3, eANT –mixture 1a, H_4eANT , H_6eANT –mixture 1b'–1b''' dimeric type compounds of eAN, eAQ and eANT –mixture 3a–3d.

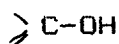
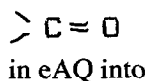
2.5. Parameters characteristic for the course of deep hydrogenation

It was convenient to introduce parameter β

$$\beta = n_{H_2}^t / n_{eAQ}^0$$

where: $n_{H_2}^t$ –the number of hydrogen moles consumed up to time t , n_{eAQ}^0 –the initial number of eAQ in the reactor.

Within the range $0 < \beta < 1$ hydrogenation was fast, and $\beta = 1$ was reached in 3–6 min. Hence it has been assumed that within $0 < \beta < 1$ only hydrogenation of



i.e. formation of $eAQH_2$ proceeded (stage 'a') which was confirmed using TLC analysis. It was stated earlier [11,12] that reaction 1 proceeds quantitatively only at high amount of Pd/SiO₂ catalyst. On the other hand in the presence of

Raney–Ni [16,17,21,22] as well as low concentration of Pd/SiO₂–Al₂O₃ catalyst [23,24] a small amount of side products was formed.

At $\beta > 1$ the next reaction step termed 'deep hydrogenation' begins, in which the formation of H_4eAQH_2 initially predominates. All other products formed are denoted as 'degradation products'. $eAQH_2$ and H_4eAQH_2 react easily and quantitatively with oxygen to give corresponding quinones eAQ and H_4eAQ . In the oxidized solution normally used for analyses the quinols are absent and only the corresponding quinones are present.

For reaction carried out at $\beta > 1$ the results of HPLC were expressed as

$n_{eAQH_2}^t$ –number of eAQH₂ moles at time t
(equal to n_{eAQ}^t after oxidation)

$n_{H_4eAQH_2}^t$ –number of H_4eAQH_2 moles at time t
(equal to $n_{H_4eAQ}^t$ after oxidation)

Subsequently the following parameters were calculated: the percentage total conversion (X_c) of eAQH₂:

$$\%X_c = (n_{eAQH_2}^0 - n_{eAQH_2}^t / n_{eAQH_2}^0) \cdot 100$$

the percentage yield (Y) of H_4eAQH_2 :

$$\%Y = (n_{H_4eAQH_2}^t / n_{eAQH_2}^0) \cdot 100$$

the percentage degradation (X_d) of eAQH₂:

the average degree of hydrogenation (U) of degradation products:

$$U = n_{\text{H}_2}^t - n_{\text{H}_2}^0 - n_{\text{H}_2}^s / n_d^t$$

where:

n_d^t – number of moles of degradation products

$n_{\text{H}_2}^t$ – total number of hydrogen moles consumed from the beginning of the experiment up to time t

$n_{\text{H}_2}^0$ – number of hydrogen moles consumed for the formation of $n_{\text{eAQH}_2}^0$ mol

$n_{\text{H}_2}^s$ – number of hydrogen moles consumed for the formation of $n_{\text{H}_4\text{eAQH}_2}^t$ mol

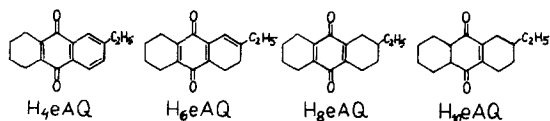
The ‘degradation products’ comprise products more deeply hydrogenated than H_4eAQH_2 (H_6eAQH_2 , H_8eAQH_2) and also possibly some products containing less hydrogen (eAN, eANT). The value of U can therefore change within a wide range.

3. Results and discussion

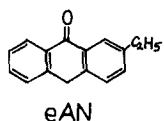
3.1. Reaction pattern

Products formed in the course of ‘deep hydrogenation’ of eAQ over Pd/SiO₂ catalyst can be arranged into four groups:

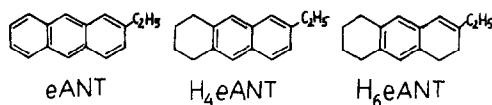
Group I: compounds in which aromatic rings in eAQ are partly or completely hydrogenated without cleavage of carbon–oxygen bond.



Group II: compounds in which one carbon–oxygen bond is cleaved, represented by only one product.



Group III: compounds in which both carbon–oxygen bonds are cleaved, and in addition aromatic rings are hydrogenated.

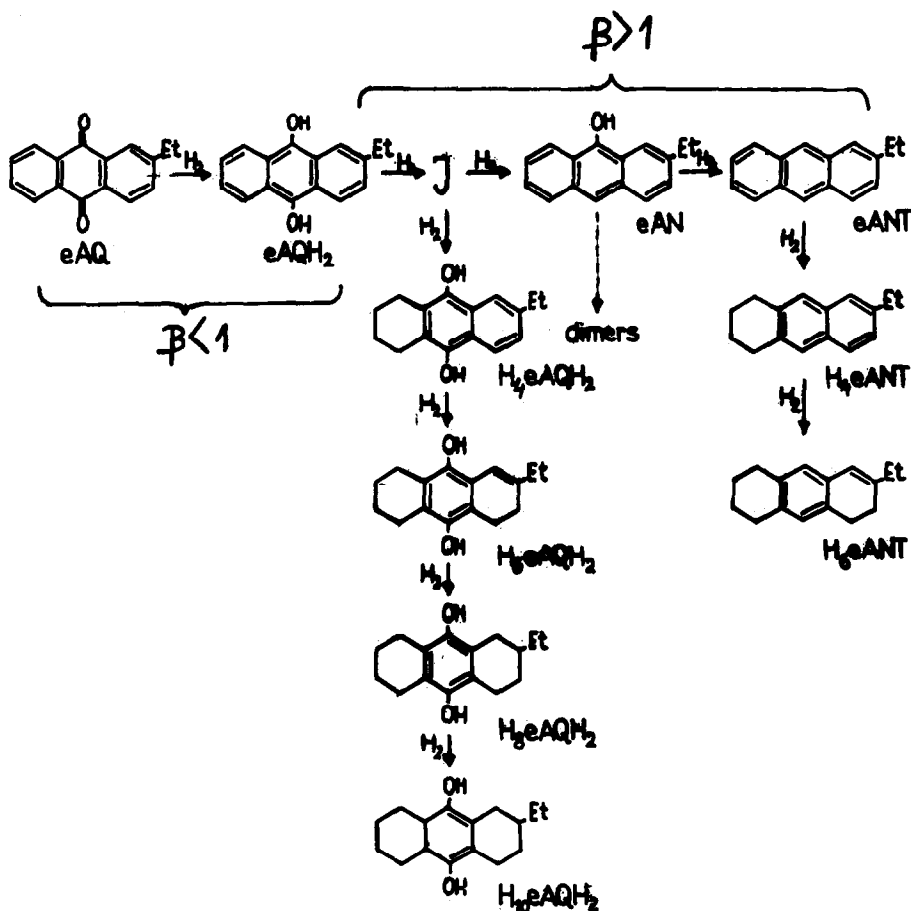


Group IV: compounds not exactly identified, similar to those formed in eAN hydrogenation. Most probably they contain different dimeric products.

The presence of these types of compounds indicates that both hydrogenation and hydrogenolysis proceed in our system. The plausible reaction pattern is presented in Scheme 2. In this Scheme only the formulas of identified products are marked. Similar compounds were detected among the products of high pressure readdition of anthraquinone (H_4 , H_6 , H_8 – derivatives) and anthrone (H_4 – H_{10} – derivatives of anthrone and anthracene) over Pt or Ni catalysts [10,14,15].

Kinetic data discussed in the previous paper [11] indicated that H_4eAQH_2 was formed in a consecutive reaction – by an unidentified intermediate product I. The reduction of AQ to AN with lithium hydride proceeded also in a consecutive reaction [10,25] – via 9,10-dihydro-9,10-dihydroxyanthracene. This compound was separated and identified by Boyland [26]. An analogous compound might be the postulated intermediate for the eAN (see Scheme 2) formation. However, for the formation of H_4eAQH_2 , rather its isomer containing also two H atoms but situated on the aromatic ring should be suggested. In such a case the diagram should include two intermediates initiating both further reaction routes.

The course of two main reaction routes was confirmed by the study of hydrogenation of pure eAN and H_4eAQ . At the same conditions the rate (r_{H_2}) of H_4eAQ hydrogenation was lower and that of eAN higher. The main products formed in hydrogenation of eAN and H_4eAQ were eANT and H_8eAQ resp. besides which different side products were also found (TLC). The number of



side products formed in particular cases was different. Hydrogenation of H_4eAQ proceeded more selectively. In the IR spectrum of its products besides the $C=O$ band at 1657 cm^{-1} corresponding to H_4eAQ (Fig. 1) only one new $C=O$ band at 1640 cm^{-1} appeared characteristic for H_8eAQ . Simultaneously the intensities of $C-H$ aromatic bands ($700\text{--}900\text{ cm}^{-1}$) for the products are lower thus indicating that hydrogenation of aromatic ring was the predominant process. The products of H_4eAQ hydrogenolysis were not observed in accordance with results obtained in the course of H_4AQ hydrogenation [10,14].

A number of products was formed in the course of eAN reduction. In the IR spectrum of products (Fig. 2) besides the bands corresponding to unreacted eAN ($C=O$ band at 1652 cm^{-1}) and $eANT$ several new bands appeared. The intensity of bands corresponding to CH_2 groups (2980--

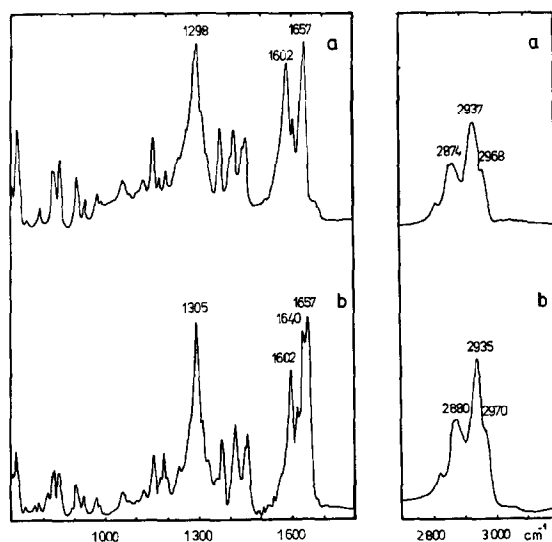


Fig. 1. IR spectrum for: (a) H_4eAQ , (b) products of H_4eAQ hydrogenation (only a part of substrate was consumed in reaction). Conditions: 0.9 g of catalyst ($d = 0.0675\text{ mm}$) $2.7 \cdot 10^{-3}$ mol of substrate in 30 cm^3 of solution, $T = 62^\circ\text{C}$.

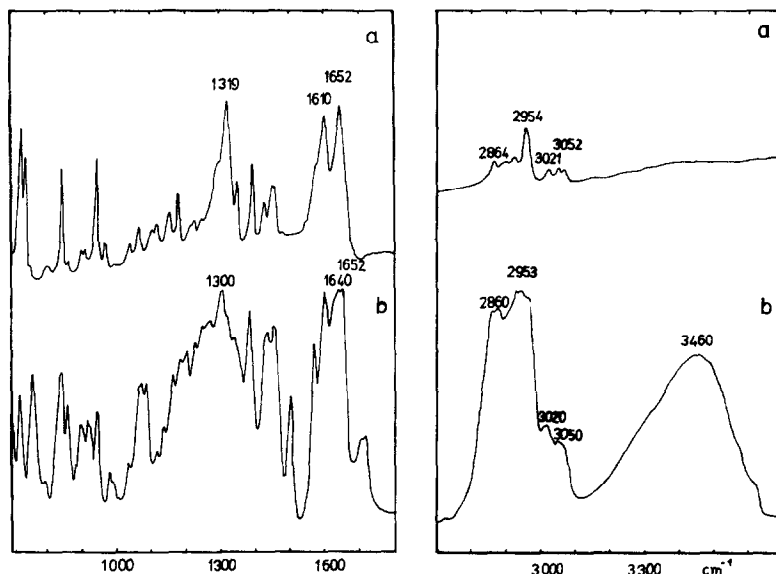


Fig. 2. IR spectrum for: (a) eAN, (b) products of eAN hydrogenation (only a part of eAN was consumed in reaction). Conditions as in Fig. 1.

2960 cm^{-1}) increases for the products thus indicating that the hydrogenation of aromatic rings in eAN proceeds in accordance to [14,27,28]. The presence of a strong band at 3460 cm^{-1} (Fig. 2) corresponding to OH groups suggests that in the course of eAN hydrogenation dimeric type compounds were formed. Very much similar IR spectra containing a band at 3460 cm^{-1} (Fig. 3) were obtained for some products of eAQ hydrogenation. For such products molecular masses as high as 450 and 410 in mass-spectrometric analysis were obtained. The first one corresponds to dimers of eAQ or H_4eAQ , the second to dimers of eANT. The formation of dimeric products was observed in the reduction of AQ and AN [10] as well as in catalytic hydrogenation of eAN over Raney-Ni [19]. In the latter case predominantly the dimer

2,2-diethyl-10,10-dihydroanthrone was formed along with only a small amount of eANT.

3.2. The regime of 'deep hydrogenation'

As Scheme 2 shows in the course of 'deep hydrogenation' parallel and consecutive reactions proceed simultaneously, all of them with the participation of hydrogen. Hence the rate of particular reactions must evidently be influenced by the concentration of hydrogen at the catalyst surface (and its availability). This concentration depends on the type of reaction regime; is high in kinetic but low in diffusion regime [3,4].

In order to determine reaction regime the change of the rate of hydrogenation (r_{H_2}) as a function of the catalyst amount m (0.3–0.9 g), its

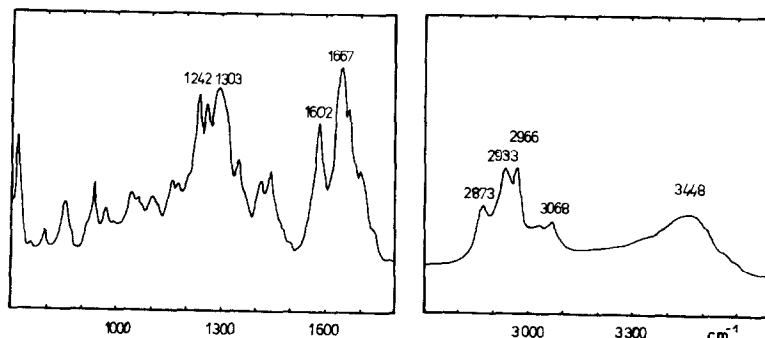


Fig. 3. IR spectrum for the products of the deep hydrogenation of eAQ; group IV of products (Scheme 1).

Table 2

The correlation between apparent activation energy, catalyst amount, grain size and conversion of eAQH₂

Catalyst amount (g)	Grain size (mm)	Conversion (%)	Temperature range (°C)	<i>E</i> (kcal/mol)	Reaction regime
0.3	0.0675	<i>X_c</i> < 70%	21–52	11.38	kinetic
			52–62	5.44	diffusion ^a
		<i>X_c</i> > 70%	21–62	8.58	mixed ^b
0.9	0.0675	<i>X_c</i> < 65%	21–44	10.64	mixed
			44–62	6.37	diffusion
		<i>X_c</i> > 65%	21–62	11.30	kinetic
0.9	0.135	<i>X_c</i> < 80%	18–51	11.88	kinetic ^c
			51–62	2.45	mass transfer
		<i>X_c</i> > 80%	18–62	9.18	mixed

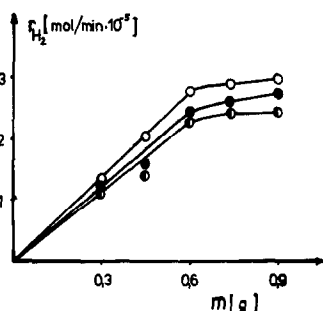
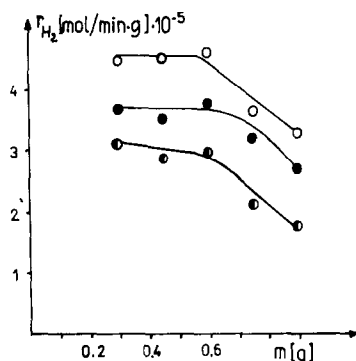
^a Internal diffusion regime.^b Mixed: the rate of chemical reactions (external catalyst surface) as well as internal diffusion influenced the overall rate^c So-called external kinetic regime.Fig. 4. The rate of hydrogen consumption (r_{H_2}) as the function of catalyst amount m ($d=0.0675$ mm) for reaction at 21°C. Total conversion, X_c , of eAQH₂ equal to: ○ - 20%, ● - 40%, ◐ - 50%.

Fig. 5. Specific catalyst activity as the function of catalyst amount (Conditions as in Fig. 4).

grain size d (0.0675–0.135 mm), reaction temperature (18–62°C) and apparent activation energy (Table 2) was considered. In particular cases also the influence of agitation frequency on r_{H_2} was investigated. The values of r_{H_2} were cal-

culated at the same total conversion (X_c) of eAQH₂.

In all experiments the same agitation frequency of the liquid was applied, high enough to eliminate the external mass transport processes at 21°C.

At 21°C r_{H_2} increases linearly with catalyst amount up to 0.6 g of catalyst (Fig. 4) and becomes practically constant for higher catalyst amounts. This means that below and at $m=0.6$ g the specific catalyst activity is constant but decreases above that value of m (Fig. 5). The size of the catalyst grain d was important only at high amount (0.9 g) of catalyst; r_{H_2} decreased with the increase of d . At small amount of catalyst ($m=0.3$ g) r_{H_2} does not depend on catalyst grain size d . However, the same values of E equal to about 11 kcal/mol were calculated for low (0.3 g) as well as for high (0.9 g) catalyst amount, high enough to indicate reaction kinetically controlled.

The linear sections of the graphs in Fig. 4 correspond to the situation in which hydrogen concentration at the catalyst surface is constant and reaches the highest possible level ('hydrogen rich mode'). Above $m=0.6$ g this hydrogen concentration is somewhat lower but the rate controlling step still remains essentially the same. The possible explanation of such result is that at the small amount of catalyst ('hydrogen rich mode') hydrogen is penetrating into the bulk of the grains

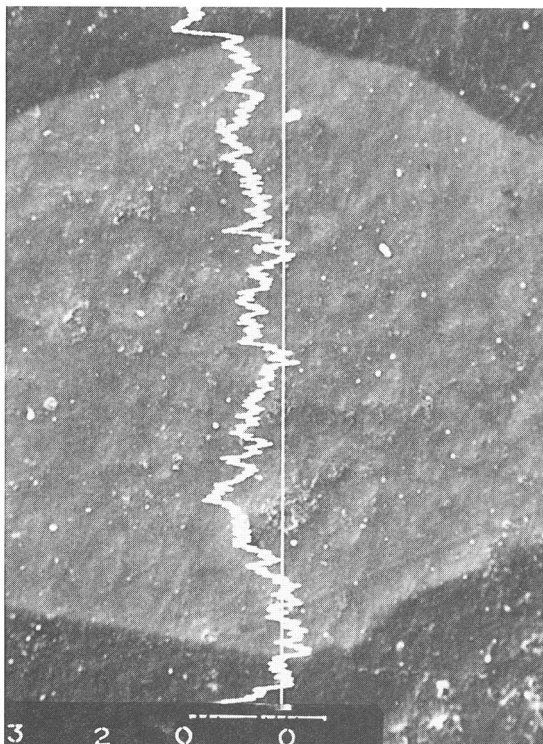


Fig. 6. Pd distribution on the external surface of the catalyst grain.

where its highest possible concentration is preserved. Consequently palladium on the external

surface as well as in the internal part (bulk) of the catalyst grains participates in the reaction. When the amount of catalyst is doubled, the catalyst is working in less rich hydrogen mode and its penetration into the deepest layers of large grains is somewhat limited. Therefore the overall activity of such grains diminishes. This is the transition (partial or total) to a so-called 'external kinetic regime' of the reaction. In the latter situation only palladium situated on the external surface of the catalyst acts in the reaction. This suggestion is in accord with the palladium distribution determined experimentally. The content of palladium was practically the same (4 wt%) for all grains regardless of their size (Table 1) and also the same palladium distribution was observed for the small as well as the large catalyst grain. The distribution of Pd on the external catalyst surface was practically uniform (Fig. 6). Fig. 7 shows that in the bulk of catalyst grains palladium was evenly distributed and only in the thin near to the surface layer its content was higher.

As Fig. 8 shows the rate of hydrogenation per gram of catalyst r_{H_2}/g (specific catalyst activity) for reaction in kinetic (curve A) and external

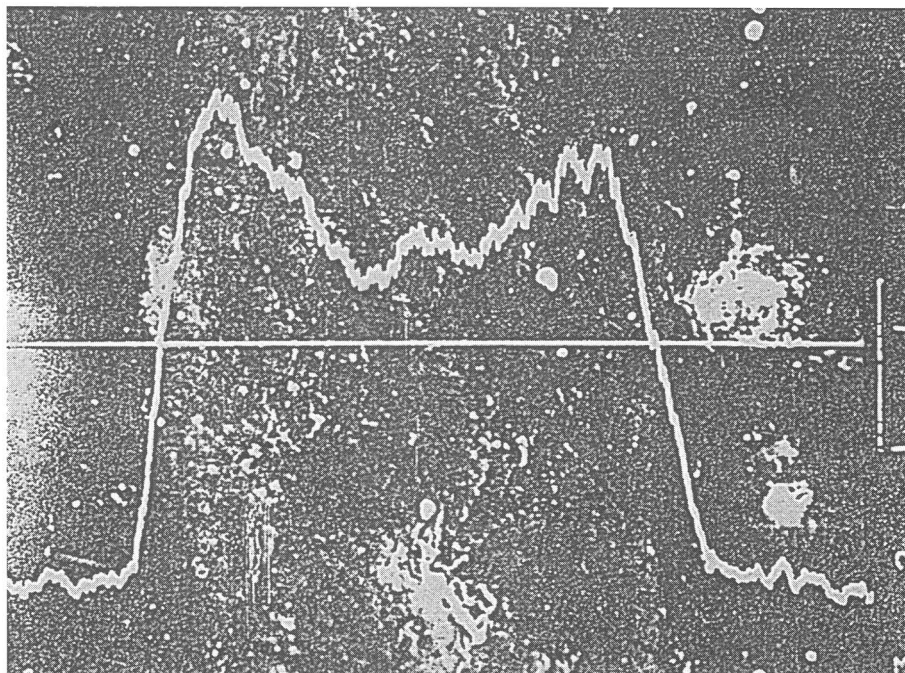


Fig. 7. Pd distribution in the cross-section of the catalyst grain.

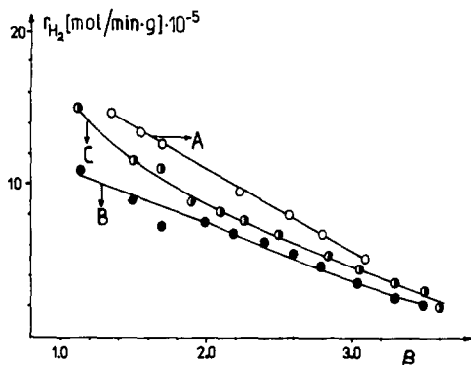


Fig. 8. Specific catalyst activity (r_{H_2} /g of catalyst) for reaction in kinetic (curve A), external kinetic (curve B) and internal diffusion (curve C) regime. Temperature of reaction 44°C.

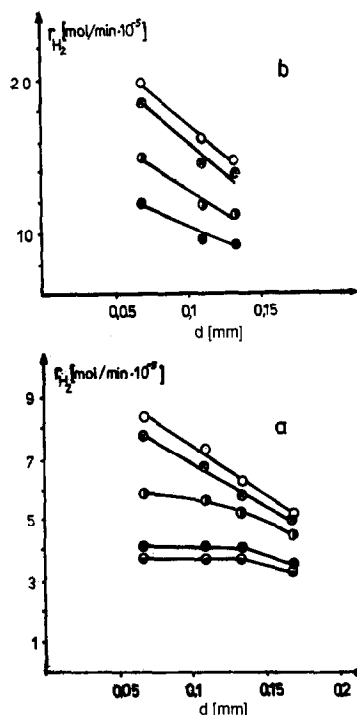


Fig. 9. The rate of hydrogen consumption (r_{H_2}) as the function of catalyst grain size (d) for reaction at 62°C and (a) 0.3 g of catalyst (b) 0.9 g of catalyst r_{H_2} calculated at the total conversion, X_c , equal to: \circ - 20%, \otimes - 30%, \bullet - 50%, \ominus - 70%, $\omin�$ - 80%.

kinetic regimes (curve B) were different, lower was r_{H_2} /g when only external catalyst surface took part in reaction.

No analogous effects due to the distribution (outside and inside) of palladium in the catalyst grains were observed in the study of the first stage (stage 'a') of eAQ hydrogenation resulting in the formation of eAQH₂ [12]. In this case the typical

correlation for the 3-phase reaction system was observed: with the increasing amount of catalyst the regime of reaction changed from a kinetic to an external mass transport one [1,3]. The observed differences in the catalyst activity in stages 'a' and 'b' may be the consequence of the dimerization or polymerization of partly hydrogenated products (in our case eAQH₂ or eAN) in stage 'b'. Such compounds may cause catalyst deactivation (stereochemical hindrance). In fact the formation of dimers in our system was observed.

The transition from kinetic to the diffusion regime of 'deep hydrogenation' has been reached by increasing reaction temperature. At 62°C r_{H_2} was depending on the agitation frequency only for catalysts with large grains ($d=0.135$ mm) at 0.3 g as well as at 0.9 g of catalyst indicating the influence of external mass transport processes. This may be the transport of reagents (most probably of hydrogen) to the catalyst surface through the liquid but not the process of hydrogen dissolution. The rate of hydrogen dissolution at the present conditions is distinctly higher (≈ 20 times) [11] than values of r_{H_2} observed in 'deep hydrogenation'. In all other cases the frequency of agitation did not influence r_{H_2} at 62°C thus indicating that external mass transport processes were eliminated. On the other side r_{H_2} depended

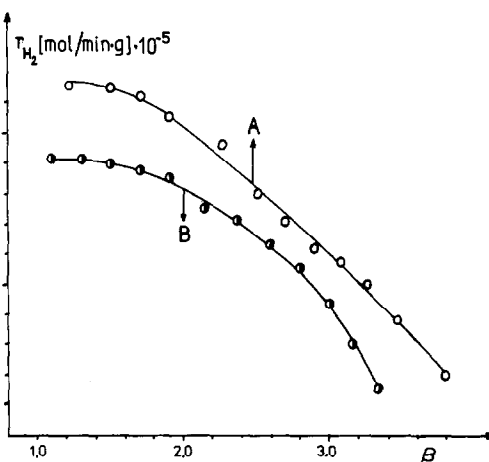


Fig. 10. Specific catalyst activity for reaction in internal diffusion (curve A) and external mass transport regime (curve B). Temperature of reaction 62°C.

on the catalyst grain size (Fig. 9) and also low values of E (Table 2) were calculated. These effects suggest that at these conditions internal diffusion process influenced the rate of chemical reaction. Fig. 10 shows that specific catalyst activity (r_{H_2}/g) was higher for reaction influenced by internal diffusion (curve A), lower than external mass transport processes controlled the rate of chemical reaction (curve B).

The increase of temperature was accompanied by different changes of the reaction regimes (Table 2):

at 0.3 g of catalyst ($d=0.0675$ mm) the reaction regime changes from kinetic at 21°C to internal diffusion at 62°C (decrease of E nearly to half of the value obtained in the kinetic regime).

at 0.9 g of catalyst $d=0.0675$ mm with the increasing temperature of reaction the internal diffusion processes becomes also gradually more and more important.

at 0.9 g of catalyst ($d=0.135$ mm) the direct transition from external kinetic at 18°C to external mass-transport regime at 62°C was observed ($E=2.45$ kcal/mol).

Hence depending on catalyst amount its grain size and temperature deep hydrogenation can be governed by external mass transport processes ($E=2.5$ kcal/mol), internal diffusion (E about 5–6 kcal/mol), surface reaction ($E>10$ kcal/mol) or may occur in the mixed control regime.

The determination of the exact nature of the diffusing species in the particular cases of reaction occurring in the diffusion regime was outside the scope of the present investigation. It should be the object of further study comprising the determination of such kinetic parameters as rate constants of particular reaction steps, hydrogen concentration in the solution etc.

As the data in Table 2 show at high values of conversion X_c (65–80%) independently of the catalyst amount correlation between r_{H_2} and the catalyst grain size d becomes less distinct (Fig. 9) and also higher values of E (at this high X_c) were obtained (11 kcal/mol). Hence the change of the reaction regime occurs in the course of reaction.

This effect can be explained if we consider that at high conversion of eAQH₂ its concentration in solution is low and hydrogen is mainly used for hydrogenation of other previously formed products (i.e. H₄eAQH₂). The rate of all such reaction is low in comparison with the rate of eAQH₂ hydrogenation and the conditions of process correspond now again to kinetically controlled reaction ('hydrogen rich mode'). On the other side the transition to the 'hydrogen rich mode' may also be the result of catalyst deactivation due to the chemisorption of some reaction products.

3.3. The influence of the reaction regime on the course of 'deep hydrogenation'

Different reaction regimes were achieved depending on the catalyst amount, catalyst grain size and reaction temperature.

In the present section the dependence of X_c , X_d , U and the yield of H₄eAQH₂ on the β parameter will be discussed in the particular types of reaction regimes as illustrated by Fig. 1.

As Scheme 2 shows H₄eAQH₂, the main product of 'deep hydrogenation' can be assumed as the intermediate compound and therefore in the course of reaction its concentration passes over a maximum (Fig. 1). The fact that 'degradation products' according to their definition may comprise the products only slightly hydrogenated as eAN (and possibly the hypothetical intermediate product I) as well as the products deeply hydrogenated results in a fairly complicated shape of the curves $X_d - \beta$ in which local maxima appear.

In the *kinetically controlled* process (Fig. 11) the maximal yield of H₄eAQH₂ was as low as only 50% and was reached at $X_c = 75\%$, i.e. before the total consumption of eAQH₂. From the beginning of reaction deeply hydrogenated degradation products were formed ($U \approx 3.5-4$) as well as eANT. The concentration of eANT was very low and its presence was stated only by TLC more sensitive than HPLC. Above results indicated that from the beginning of 'deep hydrogenation' both reaction routes: hydrogenation and hydrogenolysis occurred. The maximal value of Y was not high

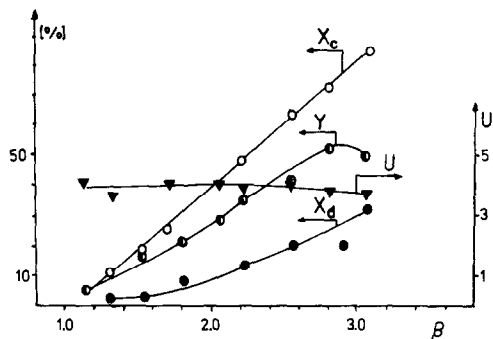


Fig. 11. The change of X_c , X_d , Y and U in the course of kinetically controlled reaction (conditions: 0.3 g of catalyst $d=0.0675$ mm, temperature 44°C).

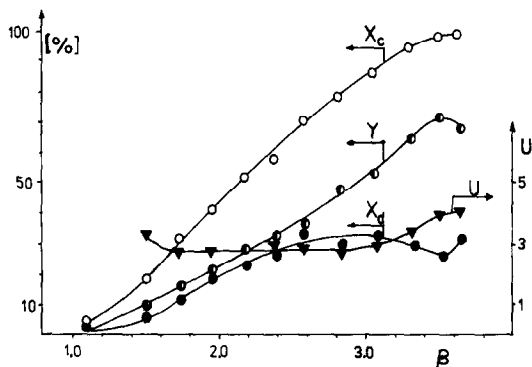


Fig. 12. The change of X_c , X_d , Y and U in the course of reaction in external kinetic regime (conditions: 0.9 g of catalyst, $d=0.135$ mm, temperature 44°C).

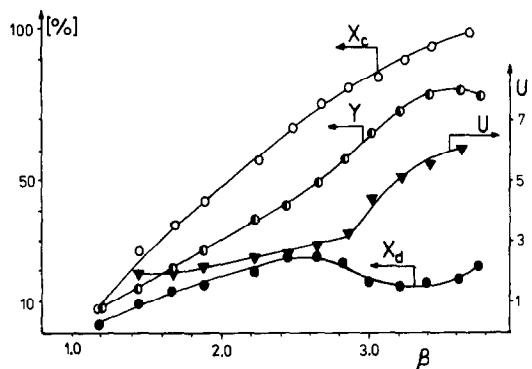


Fig. 13. The change of X_c , X_d , Y and U in the course of reaction in internal diffusion regime (conditions: 0.3 g of catalyst, $d=0.0675$ mm, temperature 62°C).

in this case which shows that further hydrogenation of H_4eAQH_2 to H_6 and H_8 derivatives was relatively fast and proceeded from the very beginning.

If we compare *kinetic* (Fig. 11) and so-called ‘external kinetic’ regimes (Fig. 12) it is seen that

at a given β value practically the same amount of eAQH_2 was converted (X_c). This effect indicates that reaction in which eAQH_2 was converted proceeded similarly in both regimes. However, the differences appeared in the course of degradation reactions and H_4eAQH_2 formation. In the ‘external kinetic’ regime the maximal yield of H_4eAQH_2 was high (equal to 72%) and reached only after the whole amount of eAQH_2 was consumed ($X_c \approx 95\%$). In this regime the percent of degraded eAQH_2 was also high, but low degree of hydrogenation of degradation product ($U \approx 3$) was observed (Fig. 12). In these reaction conditions eAN and eANT were formed in sufficiently high amounts to be detected by HPLC, indicating that the rate of hydrogenolysis was relatively high, higher than in the kinetic regime. The increase of the hydrogenolysis rate was accompanied by the decrease of the reactions rate occurring in the route comprising the hydrogenation processes (Scheme 2) and especially the hydrogenation of H_4eAQH_2 to H_6 – H_8 derivatives. It may be supposed that due to this latter effect the yield of H_4eAQH_2 was higher (Fig. 12).

As already said the diffusional regime of ‘deep hydrogenation’ was achieved by raising the temperature to 62°C .

If 0.3 g of catalyst of small grains ($d=0.0675$ mm) was used reaction was controlled by the *internal diffusion* (Fig. 13). However, at the same amount of catalyst and the same temperature but with the catalyst of much larger grain size

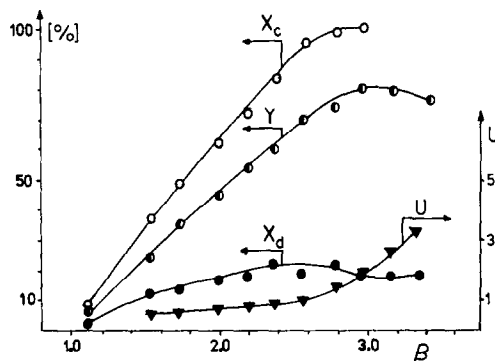


Fig. 14. The change of X_c , X_d , Y and U in the course of reaction in external mass transport regime (conditions: 0.3 g of catalyst, $d=0.135$ mm, temperature 62°C).

($d=0.135$ mm) external mass transport processes determined the overall reaction rate (Fig. 14).

Now if we compare both diffusional reaction regimes at a given value of β we state higher amount of eAQH₂ converted and larger yield of H₄eAQH₂ in external mass transport regime. On the other side the maximal yield of H₄eAQH₂ was the same in both regimes and amounted to about 80%. This maximal value was reached at the same $X_c \approx 95\%$ but at different values of β ($\beta=3$ – external mass transport regime, $\beta=3.5$ – internal diffusion regime). The percentage degradation of eAQH₂ (X_d) was only somewhat larger in internal diffusion regime. In these latter conditions deeply hydrogenated degradation products were formed ($U \approx 3$) as compared with the products formed in external mass transport regime ($U \approx 1$). As Fig. 14 shows such low hydrogenated degradation products were formed up to $X_c \approx 95\%$. After this point deeply hydrogenated degradation products appear thus showing that in this reaction regime the transformation of H₄eAQH₂ into further degradation products practically begins only after almost complete use of eAQH₂.

Somewhat different behaviour was observed in the case of internal diffusion regime (Fig. 13). Higher hydrogenated degradation products ($U=2-3$) were already formed in the early stages of the reaction and the final hydrogenation degree was very high reaching value about 6. In these conditions besides eANT the largest number of side products was formed (TLC).

A plausible explanation of these latter effects is to assume that in the internal diffusion regime prolonged contact of the substrate molecules with the catalyst surface favours deeper hydrogenation. For reaction in the external mass transport regime the number of side products was smaller but eANT and dimeric compounds were formed from the very beginning of deep hydrogenation. As was already said, dimeric compounds were predominantly formed in the course of eAN reduction. Hence it can be supposed that in the conditions when external mass transport controls the rate of chemical reaction, the hydrogenolytic degradation

process proceeds at a relatively high rate from the very beginning of reaction.

Dimeric type compounds were not observed for the kinetically controlled reaction (hydrogen rich conditions) thus indicating that in the above conditions the hydrogenolysis reaction and in particular dimerization proceeded at a much lower rate.

The author expresses her best thanks to Prof. Dr A. Bielanski for stimulating discussions, reading the manuscript and critical remarks.

References

- [1] Ch.N. Satterfield, Mass Transfer in Heterogeneous Catalysis, MIT Press, Cambridge, MA, 1970.
- [2] N.D. Kunz and T.A. Joson, Chem. Eng. Progr., 76(6) (1980) 49.
- [3] I. Horak and J. Pasek, Design of Industrial Chemical Reactors from Laboratory Data, Heyden & Son, London, 1978.
- [4] P.N. Rylander, Chem. Eng. Progr., 76(6) (1980) 46.
- [5] J.W.E. Coenen, in J.H. de Boer (Ed.), The Mechanism of Heterogeneous Catalysis, Elsevier, Amsterdam, 1959.
- [6] M. Zajcev, J. Am. Oil Chem. Soc., 37 (1960) 11.
- [7] P.N. Rylander, Catalytic Hydrogenation over Platinum Metals, Academic Press, New York, 1967.
- [8] P.N. Rylander, I.M. Karoenko and G.R. Pond, Ann. NY Acad. Sci., 172 (1970) 1266.
- [9] S.S. Scholnik, I.R. Reasenber, E. Lieber and G.B.L. Smith, J. Am. Chem. Soc., 63 (1941) 1191.
- [10] J. Houben, Das Antracen und die Anthrachinone, Georg Thieme Verlag, Leipzig, 1929.
- [11] A. Drelinkiewicz, J. Mol. Catal., 75 (1992) 321.
- [12] A. Drelinkiewicz, Bull. Pol. Acad. Sci., Ser. Chim., 39 (1991) 63.
- [13] W.W. Lunin, W.I. Bogdan, N.N. Kuzuecara and N.W. Dobroserdova, Kinet. Katal., 28 (1987) 499.
- [14] J. Braun and O. Bayer, Berichte, 58 (1925) 2667.
- [15] A. Skita, Berichte, 58 (1925) 2685.
- [16] L.H. Frejdlin and E.F. Litwin, Izv. Akad. Nauk SSSR, Otd. Khim. Nauk, 4 (1960) 734.
- [17] L.H. Frejdlin, E.F. Litwin and W.E. Dient, Dokl. Akad. Nauk SSSR, 131 (1960) 1362.
- [18] Ulmanns Encyclopedia of Industrial Chemistry, VCH, Weinheim, 17 (1969) 697.
- [19] S.W. Sjawcillo, W.I. Sawushkina and E.M. Zernowskaya, Zh. Obshch. Khim., 28 (1959) 1752.
- [20] D.T. Burns and R.K. Harle, Anal. Chim. Acta, 100 (1978) 563.
- [21] A.B. Fasman, S.D. Mikhailenko, N.A. Maksimova, Zh.A. Iksanov, V.Ya. Kitaigorodskaya and L.V. Pavlyukevich, Appl. Catal., 6 (1983) 1.
- [22] S.D. Mikhailenko, A.B. Fasman, N.A. Maksimova and E.V. Leongard, Appl. Catal., 12 (1984) 141.
- [23] Zh.A. Iksanov, V.Ya. Kitaigorodskaya, L.V. Pavyukievich, G.N. Baera, E.S. Szpiro and A.B. Fasman, Zh. Prikl. Khim., 59 (1986) 360.

- [24] E.M. Moroz, S.D. Mikhailenko, A.K. Dzhuhusov, L.V. Pavlyukievich and A.B. Fasman, *Kinet. Katal.*, 31 (1990) 1506.
- [25] A. Vogel, *Textbook of Practical Organic Chemistry*, Longman, London, 1978.
- [26] E. Boyland and D. Mauson, *J. Chem. Soc.*, (1951) 1837.
- [27] A. Skita, *Berichte*, 60 (1927) 2522.
- [28] J. Braun and O. Bayer, *Annalen*, 459 (1927) 287.